Polymer 49 (2008) 5467–5473

Contents lists available at ScienceDirect

Polymer

journal homepage: www.elsevier.com/locate/polymer

# Dynamics of unentangled cyclic and linear poly(oxyethylene) melts

Sunghyun Nam [a], Johannes Leisen [a], Victor Breedveld [b], Haskell W. Beckham [a,*]

[a] Polymer, Textile and Fiber Engineering, Georgia Institute of Technology, Atlanta, GA 30332-0295, USA
[b] Chemical and Biomolecular Engineering, Georgia Institute of Technology, Atlanta, GA 30332-0100, USA

ARTICLE INFO

*Article history:*
Received 13 July 2008
Received in revised form 9 October 2008
Accepted 13 October 2008
Available online 18 October 2008

*Keywords:*
Cyclic polymer
Self-diffusion
Poly(oxyethylene)

ABSTRACT

Monodisperse low-molecular-weight (400–1500 g/mol) cyclic poly(oxyethylene)s (CPOE)s were synthesized from linear dihydroxy-terminated poly(oxyethylene)s (LPOE)s. The self-diffusion, NMR spin–spin relaxation, and zero-shear viscosity of CPOE and LPOE, as well as linear dimethoxy-terminated poly(oxyethylene) (LPOEDE), were measured in the melt state. The self-diffusion coefficients measured at 56 °C were ordered in the following sequence: LPOEDE > CPOE > LPOE, which is in excellent agreement with NMR spin–spin relaxation and viscosity data. The slower motion of LPOE compared to LPOEDE was attributed to chain-end hydrogen bonding. Scaling relations with molecular weight and activation energies were reconciled with chain-end and topological effects.



## 1. Introduction

Polymer dynamics are governed by molecular architecture, size, and structure. Translational dynamics more strongly depend on architecture and size than on structure. At least for linear architectures, the dynamics of different molecular structures appear to follow the same power-law scaling functions of molecular weight ($M$) with the only major difference being the critical molecular weight at which the crossover takes place between the scaling laws at low $M$ and high $M$ [1]. These two power laws, derived from the well-known Rouse [2] and reptation models [3,4], describe the dependence of the self-diffusion coefficient, $D$, and the viscosity, $\eta$, on the molecular weight: $D \sim M^{\nu}$ and $\eta \sim M^{\mu}$. The Rouse model, based on the uncorrelated motion of subunits of a macromolecule, is relevant for unentangled solutions and melts and leads to scaling predictions of $\nu = -1$ and $\mu = +1$. The reptation model, based on the correlated motion of a polymer chain along a tube defined by entanglements with neighboring macromolecules, is relevant above a critical molecular weight for entanglement, $M_c$, and leads to stronger scaling predictions of $\nu = -2$ and $\mu = +3$.

As opposed to bulk translational dynamics, local dynamics are more sensitive to molecular structure. NMR transverse, or spin–spin, relaxation times ($T_2$) can be used to probe both local dynamics and overall chain translation, and have been found to be more sensitive than self-diffusion measurements to structural changes and high frequency motions [5]. For example, $M_c$ for poly(dimethylsiloxane) (PDMS) was measured as the point at which a sharp decrease in its $T_2$ occurred; the $M_c$ determined from these $T_2$ measurements agrees with the value from $\eta$ measurements, even though no such indication of $M_c$ was observed in self-diffusion measurements until much higher molecular weights [6,7].

While the reported experimental and theoretical work on the dynamics of linear and branched polymers is extensive and highly developed, the literature on cyclic polymers is incomplete with the appearance of some conflicting views. Melt dynamics have been reported only for a limited number of cyclic macromolecules. Most studies seem to have been primarily motivated by the interesting fact that rings cannot reptate in the traditional sense due to the absence of end groups. Consistent with this notion, computer simulations have shown that cycles diffuse faster than linear polymers across all sizes studied, and do not exhibit a crossover to slower, entangled dynamics [8–10]. Here we define "slower dynamics" as those characterized by higher viscosities or smaller diffusion coefficients. More recent simulations of cyclic and linear polyethylenes revealed that cycles diffuse faster than linear polymers only at high molecular weights, with a crossover to slower dynamics occurring near the entanglement molecular weight of linear chains, $M_e$ [11,12]. This crossover to slower dynamics at low molecular weights was attributed simply to the smaller size of cyclic chains compared to linear ones of the same molecular weight, which results in higher local segment densities. Consistent with these simulations, low-molecular-weight cyclic alkanes diffuse slower than linear alkanes with the same number of carbons [13]. It was noted, however, that no published simulation studies "capture the

* Corresponding author. Polymer, Textile and Fiber Engineering, Georgia Institute of Technology, 801 Ferst Drive, Atlanta, GA 30332-0295, USA. Tel.: +1 404 894 4198; fax: +1 404 894 7452.
*E-mail address:* beckham@gatech.edu (H.W. Beckham).

0032-3861/$ – see front matter © 2008 Elsevier Ltd. All rights reserved.
doi:10.1016/j.polymer.2008.10.007

existence of entanglements in the cyclic chains" [11]. Since entanglements are required for reptation, these simulations thus support the view that cycles cannot reptate. On the other hand, *experimental* studies have shown that melts of cyclic macromolecules exhibit viscoelastic behavior consistent with the presence of entanglements [14,15]. These discrepancies between theory, simulations and published experimental data on cyclic macromolecular dynamics are often noted and remain confusing [9].

An excellent example is the literature on cyclic polystyrene (PS) melt dynamics. McKenna et al. investigated cyclic PS with zero-shear viscosity ($\eta_0$) measurements across a molecular-weight range from 11 to 185 kg/mol [16]. They reported that cyclic PS exhibited nearly the same critical molecular weight for entanglement as linear PS (~40 kg/mol), and that linear and cyclic polymers exhibited a nearly identical temperature dependence of the zero-shear viscosities. For molecular weights above $M_c$, cyclic PS exhibits lower $\eta_0$ than equivalent-molecular-weight linear PS. In a later published study of creep and recovery measurements for PS, McKenna et al. [15] reported that the $M_c$ of cyclic PS was roughly double the value found for linear PS (in contrast to their earlier finding that $M_{c,linear} \approx M_{c,ring}$), and that the cyclic-PS plateau modulus is half that of linear PS.

Although the work of McKenna and co-workers is generally consistent with viscosity data collected by Roovers on cyclic polystyrene with molecular weights from 7 to 450 kg/mol [17], significant (and puzzling) differences were also apparent. For example, the Roovers data show an upturn in the viscosity for cyclic PS of 340 kg/mol so that $(\eta_0)_{ring}/(\eta_0)_{linear} \approx 1$. McKenna suggested that this upturn is related to the presence of linear impurities "since small amounts of linear chains can greatly increase the viscosity of the cycles" [18]. McKenna also noted that lower viscosities for the Roovers samples in the intermediate-molecular-weight range may be due to the presence of knotted rings which could have originated in their preparation: ring closure of a linear PS precursor in a *poor* solvent [19]. In contrast, the samples that McKenna examined were prepared by ring closure of a linear PS precursor in a *good* solvent. Knotted and linear contaminants are notoriously difficult to remove from samples of high-molecular-weight cyclic polymers.

Semlyen prepared cyclic poly(dimethylsiloxane)s and reported on their physical properties in what is undoubtedly the most complete investigation of a cyclic polymer reported to date [20]. Cyclic PDMS melt dynamics were investigated with pulsed-field-gradient (PFG) NMR and viscosity measurements across a molecular-weight range from 0.5 to 32 kg/mol [6,14,21]. Neat cyclic PDMS was found to exhibit an $M_c$ of 17 kg/mol, essentially identical to that of linear PDMS. Cyclic PDMS is also more viscous than equivalent-molecular-weight linear PDMS at low molecular weights, but exhibits a crossover in dynamics somewhat below the linear $M_e$ to be less viscous than linear PDMS at high molecular weights [21].

There have been very few studies on the dynamics of cyclic POE. The self-diffusion of a large cyclic POE ($M_n = 10$ kg/mol) in $D_2O$ was shown to be greater than that of linear POE with the same molecular weight over the entire concentration range examined. This is consistent with the smaller hydrodynamic volume of a cyclic polymer compared to a linear polymer of the same molecular weight [22]. Low-molecular-weight linear POE is expected to have complicated dynamics due to the presence of hydroxyl end groups. Using PFG NMR, Sevreugin et al. [23] observed a spectrum of diffusion coefficients for POE melts and interpreted it as the existence of dynamic hydrogen-bonded clusters with finite lifetimes. Eckert-Kastner et al. [24] also invoked clusters to explain the results from light scattering measurements on binary blends of POE (600 g/mol) and PPO (1000 g/mol). On the other hand, Appel and Fleischer [7] did not report clusters for POE (330–41 500 g/mol), as they observed no dependence of $D$ on the diffusion duration in PFG NMR measurements.

Comprehensive property data on a homologous series of cyclic polymers have been provided only for cyclic PDMS. As pointed out by Edwards and Stepto [25], "A general understanding of the relative behavior of cyclic and linear molecules is not possible on the basis of PDMS alone." Indeed, they encouraged the preparation and characterization of a different homologous series of cyclic polymers. This contribution is provided in part for this purpose. Motivated by the incomplete and sometimes contradictory data on the dynamics of cyclic polymers, we have synthesized highly pure cyclic POE (400–1500 g/mol) and examined its melt dynamics by viscosity, NMR self-diffusion and spin–spin relaxation measurements. Cyclic POE dynamics are compared with those of linear POE containing either hydroxyl or methoxyl end groups.

## 2. Experimental details

### 2.1. Materials

Unless stated otherwise, all starting materials and solvents were purchased from Aldrich and used without further purification. Dihydroxy-terminated linear poly(oxyethylene)s (LPOE, $M_n = 200$, 400, 600, 900, 1500 g/mol) were studied and also used as starting materials to prepare cyclic POEs (CPOE, $M_n = 400$, 600, 900, 1500 g/mol). Linear poly(ethylene glycol) dimethyl ethers (LPOEDE, $M_n = 250$, 500, 1000, 2000 g/mol) were examined as they are dimethoxy-terminated linear POEs, and 18-crown-6 was incorporated into the study as a small CPOE.

### 2.2. Synthesis and purification of cyclic poly(oxyethylene)

Highly pure CPOE was prepared by end-to-end coupling of linear precursors in dilute solution and application of a novel purification protocol [26]. Briefly, commercially available α,ω-dihydroxy linear poly(oxyethylene) (400, 600, 900 and 1500 g/mol) was reacted with TsCl in the presence of KOH under pseudo-high-dilution conditions in a THF/heptane (75/25 v/v) mixture. The product mixtures were purified by inclusion complexation of the linear byproducts with α-cyclodextrin. Small quantities (3–7 wt%) of cyclic byproducts, presumably larger chain-extended cycles and catenanes, were observed in some products by gel permeation chromatography (GPC). These were removed by precipitation fractionation [27] using toluene and heptane. Cyclization and purification were monitored by GPC and NMR spectroscopy. A shift in the GPC peak towards higher elution volume and the absence of a peak at low elution volumes confirmed cyclization and purification, respectively. $^1$H NMR of the cyclic product in dry DMSO-$d_6$ showed the absence of hydroxyl end groups as a triplet at 4.5 ppm. At room temperature, the pure CPOE (50–75% yields) was a clear liquid for 400 and 600 g/mol and a white waxy solid for 900 and 1500 g/mol. All pure CPOEs exhibited narrow molecular weight distributions with $M_w/M_n = 1.02$–1.05 (1.01 for LPOE).

### 2.3. DSC measurements

Differential scanning calorimetry (DSC) was conducted on a SEIKO 220C. Sample weights of 10–15 mg were sealed in aluminum pans. The sealed samples were placed in a convection oven at 60 °C for 3 min for melting, and then rapidly quenched in liquid nitrogen and placed in the DSC cell at −120 °C. The thermal program consisted of the following: heat to 100 °C at 10 °C/min (first heating), hold 5 min, cool to −120 °C at 10 °C/min, hold 5 min, heat to 100 °C at 10 °C/min (second heating). All experiments were conducted in a flowing nitrogen atmosphere (80 ml/min). The sample thermograms were baseline-corrected by subtracting the thermogram of an empty aluminum pan, measured under the same conditions. The glass transition temperature ($T_g$) was taken from

the first heating as the midpoint of the transition. The melting temperature ($T_m$) was obtained in the second heating as the maximum of the endothermic peak.

### 2.4. NMR measurements

All NMR experiments were performed on a magnetic resonance analyzer (MARAN 23 Ultra), operating at an $^1$H frequency of 23 MHz using a permanent magnet. The spectrometer was equipped with a gradient probe and a Techron gradient amplifier. A minimum of 280 mg of sample was measured in 10-mm NMR tubes at a constant temperature of 56 °C, at which temperature all POE samples are melts.

The self-diffusion coefficient, $D$, was measured using pulsed-field-gradient (PFG) NMR with a stimulated-echo sequence [28]. The relationship between echo signal intensity and PFG parameters is given by

$$I(\delta) = I(0)\exp\left\{-\gamma^2 g^2 \delta^2 \left(\Delta - \frac{\delta}{3}\right) D\right\} \quad (1)$$

where $\gamma$ is the magnetogyric ratio of the nucleus being observed ($^1$H in these experiments). The gradient pulse magnitude $g$ was set to a constant value to achieve echo attenuation below at least 20% of the original signal intensity when varying the gradient pulse duration $\delta$ from 0.5 to 3 ms in 20 increments. The largest value of $g$ was 2.28 T/m. The gradient pulse separation $\Delta$ was 100 ms, and the recycle delay was 1 s. $I(\delta)$ is the integrated peak intensity and $I(0)$ is the intensity when $\delta$ is equal to 0. The gradients were calibrated using water and its known $D$.

The transverse, or spin–spin, relaxation times ($T_2$) were determined using a standard Carr–Purcell–Meiboom–Gill (CPMG) sequence consisting of 512 echoes separated by 1 ms. A complete decay was obtained by sampling data during the echo train. A total of 32 averages were collected with a 1-s recycle delay. All data could be fitted to a single-exponential decay. The average value of two $T_2$ measurements on each POE sample is presented and analyzed with the Brereton model [5,29], which considers the shape of the transverse relaxation function to originate in the dipolar interactions of spin pairs attached to the backbones of anisotropically moving chains [30]. For unentangled dynamics that can be described by the Rouse model, the spin–spin relaxation rate is a logarithmic function of molecular weight [31,32]:

$$\frac{1}{T_2} = \frac{6\Delta_b^2 \tau}{\pi}(\ln M_n - \ln N_a m) \quad (2)$$

where $\Delta_b$ is the dipolar interaction strength, $\tau$ is the fundamental Rouse relaxation time, $N_a$ is the number of repeat units per Rouse segment, and $m$ is the repeat unit molecular weight. A plot of $1/T_2$ versus $\ln M_n$ will have a slope of $6\Delta_b^2\tau/\pi$ and an intercept of $-(6\Delta_b^2\tau/\pi)(\ln N_a m)$; thus, the ratio of intercept to slope $= -(\ln N_a m)$ so that $N_a$ is easily determined. This value is then used in the following equation to calculate $\Delta_b$:

$$\Delta_b = \frac{\gamma^2 \hbar \mu_0}{8\pi N_a d^3} \quad (3)$$

where $\gamma$ is the magnetogyric ratio (for $^1$Hs, $26.8 \times 10^7$ sA/kg), $\hbar$ is the reduced Planck constant ($1.05 \times 10^{-34}$ m$^2$ kg/s), $\mu_0$ is the magnetic constant ($4\pi \times 10^{-7}$ m kg/s$^2$ A$^2$), and $d$ is the interproton distance (1.76 Å for POE [31]). Finally, $\Delta_b$ is used with the slope to determine $\tau$.

### 2.5. Viscosity measurements

The $\eta$ was measured with a Compact Rheometer MCR 300 from Anton Paar using a cone and plate geometry. The diameter and angle of the stainless steel cone were 25 mm and 2°, respectively, with a sample volume of 140 μl. The viscosities of all samples were found to be constant for shear rates from 5 to 300 s$^{-1}$, and the zero-shear viscosity for each sample was therefore determined as the average of five $\eta$ values at different shear rates. The measurements were carried out at 56 °C to enable direct comparison with the NMR data, and additional measurements were performed at 47, 64, and 73 °C to obtain apparent activation energies, $E_a$, for the viscosity. Duplicate measurements were performed and their average is presented.

## 3. Results and discussion

### 3.1. Thermal behavior

With the exception of the purely amorphous 400 g/mol CPOE, all of the POE samples are semicrystalline and exhibit glass, cold crystallization, and melting transitions. The glass transition temperatures ($T_g$s) and melting temperatures ($T_m$s) are shown in Table 1. The melting temperatures of both linear POEs are comparable for a given molecular weight and greater than the $T_m$s for the respective CPOEs. For a given molecular weight, the CPOE $T_g$s are just slightly greater than the LPOE $T_g$s, which are greater than the LPOEDE $T_g$s. The $T_g$s decrease with decreasing molecular weight for both linear and cyclic POEs, which is consistent with reported $T_g$s on cyclic and linear PS [33], but inconsistent with the reported $T_g$s for cyclic and linear PDMS [34]. The $T_g$s for cyclic PDMS increase with decreasing molecular weight [34,35]. Configurational entropy considerations were used to predict the molecular-weight dependence of the $T_g$s for cyclic and linear polymers by Di Marzio and Guttman [36]. They found that "whereas linear chains always show a decrease in $T_g$ as we lower the molecular weight, $x$, ring polymers either show a smaller decrease or more usually an increase in $T_g$." In their approach, whether a given ring polymer exhibits a decrease or increase in $T_g$ with decreasing molecular weight depends on the ratio between some structure-dependent local energies [36]. While it is interesting that the results on CPOE are more consistent with cyclic PS than with cyclic PDMS, it is noted that calorimetric $T_g$ measurements may be affected by polydispersity [33] and crystallinity of a given sample. In the following, melt dynamics are described for these POEs at temperatures that are at least 100 K above the POE $T_g$s.

### 3.2. Self-diffusion

Typical echo attenuation plots, $\ln[I(\delta)/I(0)]$ versus $\delta^2(\Delta - \delta/3)/10^6$, are shown in Fig. 1 for CPOE and LPOE (900 g/mol). As signified

**Table 1**
Glass transition temperature ($T_g$) and melting temperature ($T_m$) for CPOE, LPOE and LPOEDE.[a]

| Sample | Molecular weight (g/mol) | $T_g$ (°C) | $T_m$ (°C) |
|---|---|---|---|
| LPOE | 300 | −74 | −14 |
| LPOE | 400 | −71 | 7 |
| LPOE | 600 | −68 | 25 |
| LPOE | 900 | −65 | 38 |
| LPOE | 1500 | −63 | 54 |
| CPOE | 400 | −69 | – |
| CPOE | 600 | −66 | 13 |
| CPOE | 900 | −63 | 32 |
| CPOE | 1500 | −60 | 49 |
| LPOEDE | 500 | −83 | 16 |
| LPOEDE | 1000 | −71 | 40 |
| LPOEDE | 2000 | −67 | 57 |

[a] Error: $T_g \pm 1$ °C; $T_m \pm 2$ °C.

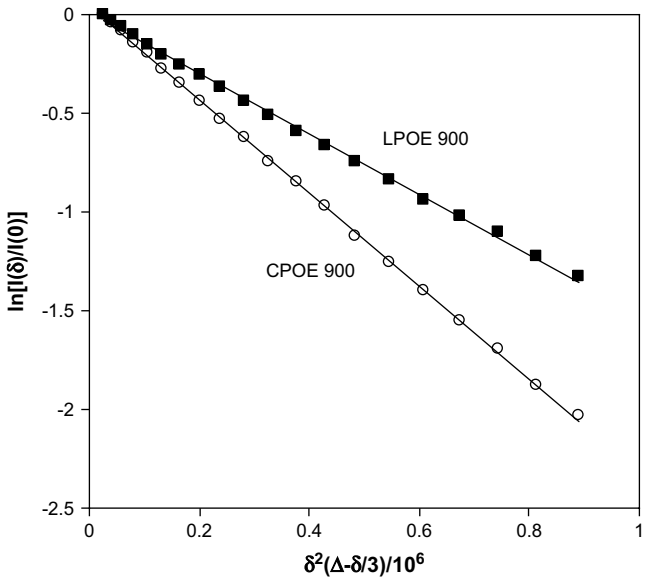


**Fig. 1.** Echo attenuation plots for CPOE (○) and LPOE (■) (900 g/mol) measured at 56 °C and $g = 1.22$ T/m. The solid lines are fits to Equation (1) from which $D$ values of $2.08 \times 10^{-11}$ m$^2$/s for CPOE and $1.37 \times 10^{-11}$ m$^2$/s for LPOE were determined.

by the slower decay, the diffusion of LPOE is slower than CPOE at this molecular weight. Straight lines, signifying single-exponential decays, were exhibited by all samples in this study. No deviations from Equation (1) were observed.

The molecular-weight dependence of the $D$ for CPOE, LPOE, and LPOEDE measured at 56 °C is shown in Fig. 2. At the same molecular weights, LPOEDE diffuses faster than CPOE which in turn diffuses faster than LPOE. Considering only topology and not chain ends, the slower diffusion of CPOE compared to LPOEDE agrees with diffusion data on low-molecular-weight cyclic alkanes [13], whose $D$s are smaller than those of corresponding linear chains. Ozisik et al. [11] suggested that the molecular and segmental motions of cyclic chains at low molecular weights are retarded as a result of high local densities due to their smaller size compared to linear chains.

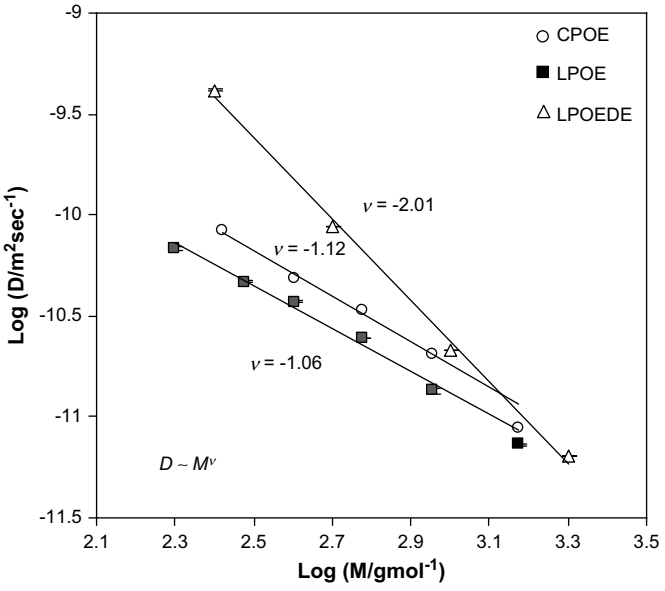


**Fig. 2.** Self-diffusion coefficients of CPOE, LPOE and LPOEDE melts versus molecular weight measured at 56 °C. Data are not corrected to iso-free volume conditions.

The radius of gyration of cyclic chains in the melt has been calculated to scale with ring size according to a power-law exponent of 0.42–0.45, compared to 0.5–0.53 for linear chains [8–10,12]. The absence of free chain ends leads to a slowdown in the dynamics of the cycles. The importance of chain ends for these low-molecular-weight polymers is further evidenced by the retarded dynamics of LPOE, whose chain-end hydroxyl groups can form intermolecular hydrogen bonds that hinder chain motion. At increasing molecular weights, the chain ends become diluted and their contribution to the overall chain motion is mitigated. This is revealed in the diffusion data of Fig. 2 as the $D$ values for LPOE and LPOEDE converge.

The $M_c$ of LPOE for transition to reptation scaling, $D \sim M^{-2}$, has been reported to occur between 2 and 3 kg/mol by PFG NMR [7,23] and at 3.6 kg/mol by viscosity measurements [37]. Since our POE samples are below these $M_c$ values, all samples are considered to be unentangled and in the Rouse regime. The scaling exponents shown in Fig. 2 are not uniformly consistent with Rouse scaling, which is $\nu = -1$ in $D \sim M^{\nu}$. The scaling exponent for LPOE in the molecular weight range of 200–900 g/mol is $\nu = -1.06$, which places LPOE for this molecular-weight range clearly in the Rouse regime. For CPOE, $\nu = -1.12$, consistent with the Rouse model. With increasing molecular weight, the $D$s exhibited a gradually stronger dependence on the molecular weight, reflected in a gradual decrease in the scaling exponents. We show this in the data of Fig. 2 by not including the highest molecular weight, 1500 g/mol, in the determination of scaling exponents for LPOE and CPOE. The $D$s for the 1500 g/mol LPOE and CPOE lie below the linear regression used to determine the scaling exponents for these two samples.

Rouse scaling was also observed for low-molecular-weight cyclic polyethylene in molecular dynamics simulations [12]. For cyclic alkanes, however, $\nu = -2.34$ was exhibited at 338 K in diffusion measurements [13]. This steep slope was explained by invoking topological constraints and highly rigid conformer structures [13]. Cyclic PDMS exhibited $\nu = -1$ over a very broad molecular-weight range [6]. The flexibility of cyclic chains, therefore, may influence the molecular-weight dependence of $D$.

While LPOE and CPOE exhibit Rouse scaling, at least over some portion of the molecular range reported, LPOEDE does not with $\nu = -2.01$. This relatively steep slope has been observed for some other linear polymers below $M_c$ [38–42], but Rouse behavior is generally recovered after correcting for free volume effects [38,39]. As the free volume is inextricably linked to the monomeric friction factor ($\zeta$), its effects on dynamics data may be eliminated by taking the product of $D$ and $\eta$, which depend inversely and directly, respectively, on $\zeta$. As will be shown later, $\eta D$ is nearly constant for LPOEDE over the molecular weight range examined, indicating adherence to the Rouse model.

### 3.3. Spin–spin relaxation

Spin–spin relaxation times, $T_2$s, were measured at 56 °C for CPOE, LPOE and LPOEDE as a function of molecular weight (see Fig. 3(a)). The $T_2$s for all POEs generally decrease with increasing molecular weight, signifying increased dipolar interactions, which is consistent with the reduction of the self-diffusion coefficients observed in Fig. 2. A similar molecular-weight dependence for $T_2$ has been observed for other low-molecular-weight polymer melts [5,6]. At the same molecular weight, $T_2$ values for LPOEDE are much higher than those for both CPOE and LPOE, which are similar to each other. For LPOEDE, the local motion of its free chain ends and high frequency rotations of methyl groups contribute to its high $T_2$ values. These chain-end effects are clearly indicated in Fig. 3(a) as the LPOEDE $T_2$ increases with decreasing molecular weight (and thus increasing chain-end concentration) at a greater rate than the $T_2$s for the other two POEs. At molecular weights greater than about

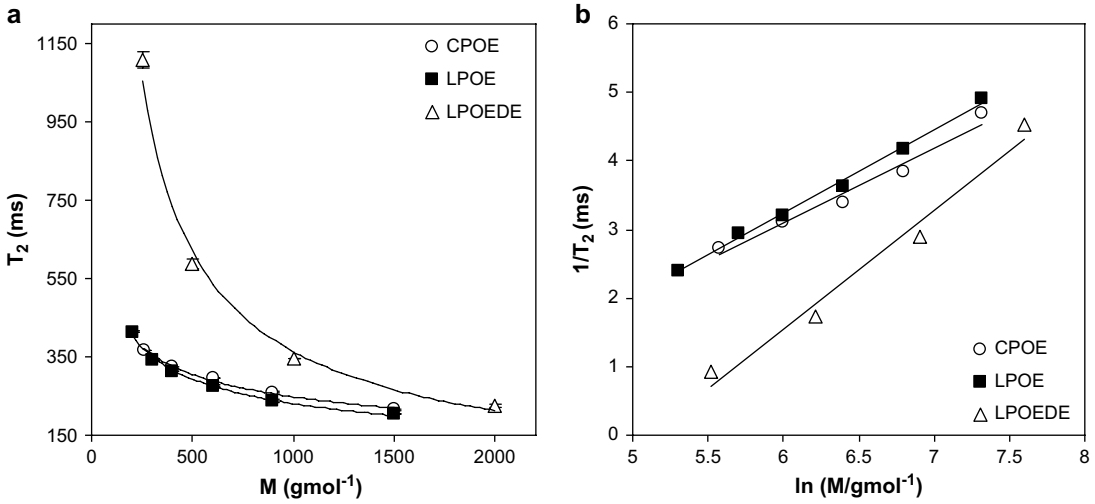


**Fig. 3.** (a) Spin–spin relaxation time, $T_2$, and (b) spin–spin relaxation rate, $1/T_2$, for CPOE, LPOE and LPOEDE versus molecular weight at 56 °C. Straight-line fits are shown for the rate data from which the slopes and intercepts were used with Equations (2) and (3) to determine the number of monomers per Rouse segment ($N_a$), the dipolar interaction strength ($\Delta_b$), and the fundamental Rouse relaxation time ($\tau$) according to the Brereton model. Error bars are smaller than the size of the symbols.

1.5 kg/mol, the POEDE $T_2$s converge with those of the other two POEs. Although LPOE also contains free chain ends, their hydrogen bonding almost perfectly compensates for any $T_2$ increase due to the free chain ends so that the $T_2$ values are virtually the same as those for CPOE, which has no chain ends at all.

The spin–spin relaxation data were formally analyzed by the Brereton model [5,29]. Strictly speaking, this model describes $T_2$ relaxation due to motions of chains and not end groups. The end-group contribution to the total $^1$H magnetization, and therefore $T_2$ relaxation, is significant for LPOEDE, minor for LPOE, and zero for CPOE. By comparing the results for these three POE samples, it is possible to evaluate the end-group effect on the results of the analysis. The reciprocal of the $T_2$ is plotted as a function of ln $M$ in Fig. 3(b). For this molecular weight range, the data for all three POEs are straight lines, confirming that the dynamics can be described by the Rouse model. The slopes and intercepts were used with Equations (2) and (3) to compute the number of monomers per Rouse segment ($N_a$), the dipolar interaction strength ($\Delta_b$), and the fundamental Rouse relaxation time ($\tau$). These quantities are shown in Table 2 for the three POEs examined in this study along with some taken from the literature for another low-molecular-weight poly(oxyethylene).

The Brereton analysis yielded results for CPOE and LPOE that are comparable, consistent with the observed $T_2$ behavior in Fig. 3. The $N_a$ values correspond to 1–2 backbone bonds, and the fundamental Rouse relaxation times are $\sim 10^{-11}$ s at 56 °C. These results are in reasonable agreement with those reported previously by Ries et al. for poly(ethylene oxide) (PEO) with unspecified end groups: 3–4 bonds comprise a Rouse segment whose relaxation time is about $3.8 \times 10^{-10}$ s [31]. Ries et al. also showed, interestingly, that the size of the Rouse statistical subunit for PEO was affected neither by temperature, nor by the addition of salt to the melt. While the PEO end groups were not explicitly discussed or specified in that report, Ries et al. have acknowledged that end groups can significantly affect the ability to extract characteristic quantitative information from $^1$H NMR transverse relaxation data, at least for crosslinked or entangled networks [30]. Rapidly moving segments such as chain ends exhibit long $T_2$ decays that can screen the faster decays characteristic of internal chain segments. The CPOE has no end groups and the ends of the LPOE chains are tied up by hydrogen bonding. The effect of the end groups on the $T_2$ data for the dimethoxy-terminated LPOEDE has already been discussed and leads to the differences in the values shown in Table 2. For LPOEDE, the number of monomers per Rouse segment is 4 and the fundamental Rouse relaxation time is $3 \times 10^{-9}$ s, which are significantly larger than the values computed for the CPOE and LPOE. The previously reported Brereton parameters for PEO lie between those for CPOE/LPOE and LPOEDE. Based on these data, one could surmise that the PEO contains one hydroxyl and one methoxyl end group per chain, which is conceivable as those end groups are the result of a very common synthesis method for poly(oxyethylene)s. Taken together, this formal analysis reveals the importance of end groups in governing the melt structure and dynamics for low-molecular-weight polymers.

**Table 2**
Results from Brereton analysis of $T_2$ data on low-molecular-weight poly(oxyethylene)s.

| Polymer | $M_n$ (g/mol) | Temp (°C) | $N_a$ | $\Delta_b$ (kHz) | $\tau$ (s) | Ref. |
|---|---|---|---|---|---|---|
| CPOE | 264–1500 | 56 | 0.50 | 140 | $3.0 \times 10^{-11}$ | – |
| LPOE | 200–1500 | 56 | 0.69 | 100 | $6.3 \times 10^{-11}$ | – |
| LPOEDE | 250–2000 | 56 | 4.0 | 17 | $3.0 \times 10^{-9}$ | – |
| PEO[a] | 600–3400 | ~56 | 1.15 | 60 | $3.8 \times 10^{-10}$ | [31] |

[a] Poly(ethylene oxide) with unspecified end groups.

### 3.4. Viscosity

Fig. 4 shows the molecular-weight dependence of the viscosity ($\eta$) for CPOE, LPOE and LPOEDE measured at 56 °C. In excellent agreement with the self-diffusion data, the CPOE viscosity is lower than that of LPOE and higher than that of LPOEDE at the same molecular weight. The viscosity differences decrease with increasing molecular weight and approach convergence above 1500 g/mol. The LPOE exhibits the highest viscosity due to hydrogen bonding, and the CPOE exhibits a higher viscosity than the LPOEDE due to its higher packing density. These results are consistent with those observed for low-molecular-weight PDMS: cyclic topologies exhibit higher viscosities than linear topologies that contain end groups incapable of strong interactions (i.e., trimethylsilyl groups) [21]. For PDMS, there is a crossover in the viscosity at a molecular weight below $M_c$ (which is the same for cyclic and linear PDMS), above which the viscosity of cyclic PDMS is lower than that of linear PDMS. The faster motion of a cyclic polymer at high molecular

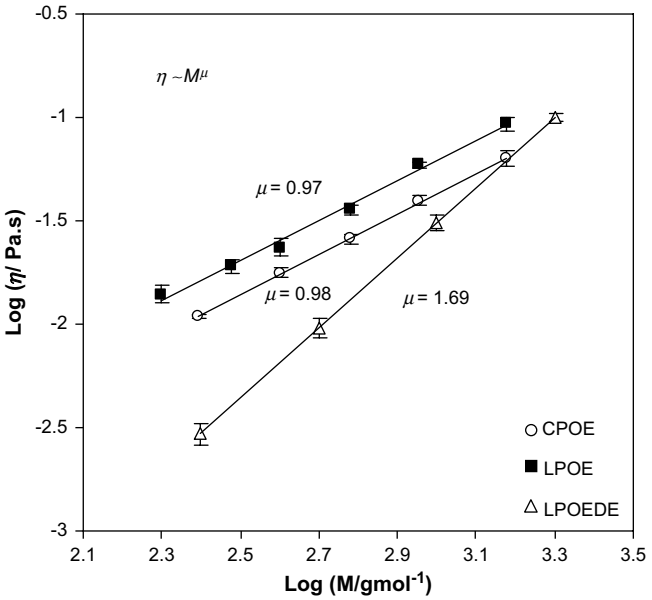


**Fig. 4.** Viscosity of CPOE, LPOE and LPOEDE melts versus molecular weight at 56 °C. Data are not corrected to iso-free volume conditions.

weights has been ascribed to less entanglements compared to a linear polymer due to its smaller size [11].

The scaling exponents for CPOE and LPOE ($\mu$ in $\eta \sim M^{\mu}$) are approximately $\mu = 1$, which is characteristic of Rouse scaling. In contrast to CPOE and LPOE, LPOEDE exhibits a $\mu = 1.69$, which is greater than that predicted by the Rouse model. Such high-molecular-weight dependencies of the viscosity below their $M_c$s have also been observed for PE ($\mu = 1.8$) [40] and for PS ($\mu \approx 1.5$) [17]. As discussed for the diffusion data, this is attributed to the presence of end groups with significant contributions to free volume. This end-group contribution is clearly diminished with increasing molecular weight as the concentration of end groups decreases. When end groups are removed, as with CPOE, the viscosity scales with molecular weight almost perfectly as predicted by the Rouse model ($\mu \approx 1$).

The ratio of the bulk viscosities of CPOE to LPOE, $\eta_{CPOE}/\eta_{LPOE}$, is approximately constant at 0.66 ($\pm$0.02). This ratio is exactly that predicted for the ratio of intrinsic viscosities for rings and chains at theta conditions [43]. Thus, the hydrogen bonding of the LPOE chain ends eliminates the $M$-dependent chain-end effect on the viscosity, but does not perturb the chain configurations. In contrast, the ratio of the bulk viscosities of CPOE to LPOEDE, $\eta_{CPOE}/\eta_{LPOEDE}$, is 4 at ~250 g/mol and decreases smoothly to 1 at ~1500 g/mol, similar to the behavior exhibited for cyclic and linear PDMS and consistent with the fact that the linear PDMS contained non-hydrogen-bonding trimethylsilyl end groups [21].

### 3.5. The product of η and D

The viscosity and self-diffusion data are consistent for the three POEs examined in this study. This is perhaps not surprising as they both depend on the monomeric friction factor, $\zeta$. According to the Rouse model [2,40],

$$\eta_{\text{Rouse}} = \frac{n\rho R_g^2 N_A \zeta}{6M} \tag{4}$$

$$D_{\text{Rouse}} = \frac{RT}{nN_A\zeta} \tag{5}$$

where $n$ is the number of repeat units per chain, $\rho$ is the density, $R_g^2$ is the mean-square radius of gyration, $N_A$ is Avogadro's number, $M$ is the molecular weight, $R$ is the universal gas constant, and $T$ is the temperature. Since $\zeta$ can be highly influenced by chain-end effects (e.g., free volume) and temperature, it can be useful for testing molecular theories to eliminate it by taking the product of $\eta$ and $D$:

$$(\eta D)_{\text{Rouse}} = \frac{\rho RT}{6}\left(\frac{R_g^2}{M}\right) \tag{6}$$

If the changes in $\rho$ and $R_g^2/M$ with molecular weight are only a minor contribution to the $\eta$ scaling, $\eta D$ should be nearly constant at low molecular weights. Pearson et al. [40] measured $\eta$ and $D$ of linear polyethylene and found that the product $\eta D$ was nearly constant below $M_c$, and then increased with molecular weight beyond $M_c$. Similar approaches and findings have been reported for polyisoprene [44] and polybutadiene [45].

Fig. 5 presents the $\eta D$ for CPOE, LPOE and LPOEDE as a function of molecular weight. The $\eta D$ values for all three POE samples are comparable (note the linear scale in Fig. 5, in contrast with the logarithmic scale of Figs. 2 and 4); a very slight decrease with increasing molecular weight can be seen for all samples, consistent with Rouse behavior. The minor decrease is attributed to small changes in $\rho$ and $R_g^2/M$ for these low molecular weights.

### 3.6. Activation energy for bulk dynamics

To investigate the temperature dependence of the flow behavior, the viscosity was measured for each sample at several temperatures between 47 and 73 °C; the lower limit was chosen so that all samples were in the liquid state. For all samples, the viscosities decreased with increasing temperature ($T$). Plots of ln $\eta$ versus $1/T$ were linear with slopes that yielded apparent activation energies, $E_a$, following use of the Arrhenius equation. The apparent activation energies are shown in Fig. 6 for CPOE, LPOE, and LPOEDE as a function of molecular weight.

The activation energies for CPOE and LPOE are similar and exhibit very little change across the entire molecular-weight range studied. At the lower molecular weights, the CPOE $E_a$ is slightly smaller than

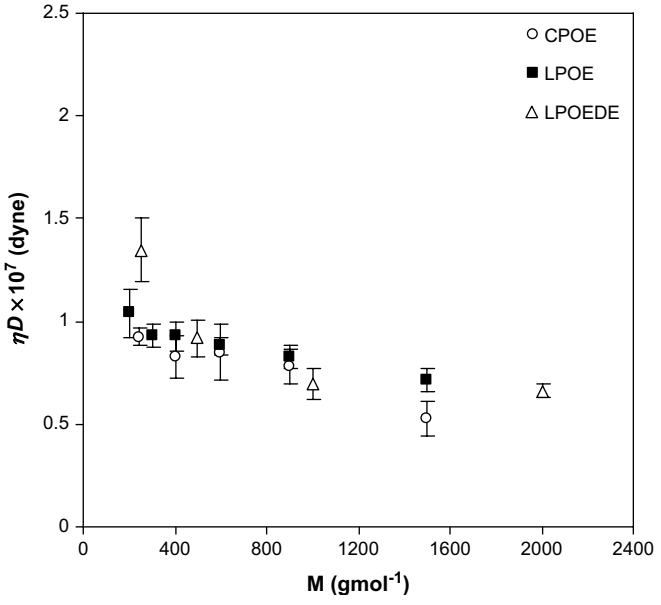


**Fig. 5.** Product $\eta D$ as a function of molecular weight for CPOE, LPOE and LPOEDE measured at 56 °C.

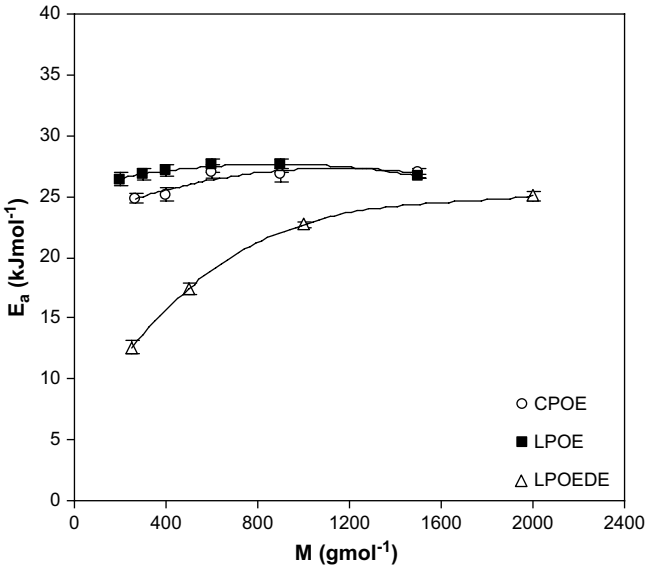


**Fig. 6.** Apparent activation energy, $E_a$, of viscosity for CPOE, LPOE and LPOEDE versus molecular weight. Viscosities were measured between 47 and 73 °C and analyzed using the Arrhenius equation.

the LPOE $E_a$. For LPOE, the activation energies show excellent agreement with a previously reported $E_a$ of 26 kJ/mol [46], which was obtained from self-diffusion measurements by PFG NMR.

In contrast, the activation energy for LPOEDE is approximately half of the CPOE/LPOE $E_a$ at ~200 g/mol, and then increases with increasing molecular weight to approach very near the CPOE/LPOE $E_a$. The behavior of the LPOEDE is clearly due to the presence of its methoxyl end groups and their attendant free volume [47]. For example, activation energies for polyisoprene self-diffusion are independent of molecular weight above 1 kg/mol [44], but exhibit a marked molecular-weight dependence below 1 kg/mol that has been attributed to increasing chain-end free volume with decreasing molecular weight. The suppression of chain-end free volume by hydrogen bonds in LPOE, and absence of chain-end free volume in CPOE eliminate the molecular-weight dependence of the activation energy in these materials.

## 4. Conclusions

Self-diffusion coefficients ($D$s), spin–spin relaxation times ($T_2$s), and zero-shear viscosities ($\eta$s) were measured for low-molecular-weight (≤2 kg/mol) cyclic poly(oxyethylene) (CPOE), linear dihydroxy-terminated poly(oxyethylene) (LPOE), and linear dimethoxy-terminated poly(oxyethylene) (LPOEDE). At the same molecular weight, the three techniques revealed a consistent picture of the dynamics: LPOEDE > CPOE > LPOE. The scaling behavior of $D$, $\eta$, $1/T_2$ and $\eta D$ with molecular weight confirmed that these polymers are unentangled and can be described by the Rouse model. Topology and chain-end structure are important considerations for the dynamics of low-molecular-weight polymers.

## Acknowledgments

This work was supported in part by the National Science Foundation (DMR-0072876). We are grateful to Joyce Ferry and Dr. Leslie Gelbaum for their assistance with cyclic polymer synthesis and NMR characterization, respectively.

## References

[1] Graessley WW. Adv Polym Sci 1982;47:67–117.
[2] Rouse PE. J Chem Phys 1953;21(7):1272–80.
[3] De Gennes PG. Scaling concepts in polymer physics. Ithaca: Cornell University; 1979.
[4] Doi M, Edwards SF. The theory of polymer dynamics. London: Oxford University Press; 1986.
[5] Brereton MG, Boden N, Ward IM, Wright P. Macromolecules 1991;24:2068–74.
[6] Cosgrove T, Griffiths PC, Hollingshurst J, Richards RDC, Semlyen JA. Macromolecules 1992;25(25):6761–4.
[7] Appel M, Fleischer G. Macromolecules 1993;26(20):5520–5.
[8] Müller M, Wittmer JP, Cates ME. Phys Rev E 1996;53(5):5063–74.
[9] Brown S, Szamel G. J Chem Phys 1998;108(12):4705–8.
[10] Brown S, Szamel G. J Chem Phys 1998;109(14):6184–92.
[11] Ozisik R, von Meerwall ED, Mattice WL. Polymer 2002;43:629–35.
[12] Hur K, Winkler RG, Yoon DY. Macromolecules 2006;39:3975–7.
[13] von Meerwall E, Ozisik R, Mattice WL, Pfister PM. J Chem Phys 2003;118(8):3867–73.
[14] Orrah DJ, Semlyen JA, Ross-Murphy SB. Polymer 1988;29(8):1452–4.
[15] McKenna GB, Hostetter BJ, Hadjichristidis N, Fetters LJ, Plazek DJ. Macromolecules 1989;22(4):1834–52.
[16] McKenna GB, Hadziioannou G, Lutz G, Hild G, Strazielle C, Straupe C, et al. Macromolecules 1987;20:498–512.
[17] Roovers J. Macromolecules 1985;18:1359–61.
[18] McKenna GB, Plazek DJ. Polym Commun 1986;27:304–6.
[19] Roovers J, Toporowski PM. Macromolecules 1983;16(6):843–9.
[20] Semlyen JA, editor. Cyclic polymers. New York: Elsevier; 1986.
[21] Dodgson K, Bannister DJ, Semlyen JA. Polymer 1980;21:663–7.
[22] Griffiths PC, Stilbs P, Yu GE, Booth C. J Phys Chem 1995;99(45):16752–6.
[23] Sevreugin VA, Skirda VD, Maklakov AI. Polymer 1986;27(2):290–2.
[24] Eckert-Kastner S, Meier G, Alig I. Phys Chem Chem Phys 2003;5(15):3202–11.
[25] Edwards CJC, Stepto RFT. Comparison of properties of cyclic and linear poly-(dimethylsiloxanes). In: Semlyen JA, editor. Cyclic polymers. New York: Elsevier Applied Science; 1986. p. 135–65.
[26] Singla S, Zhao T, Beckham HW. Macromolecules 2003;36(18):6945–8.
[27] Yu GE, Sinnathamby P, Price C, Booth C. Chem Commun 1996;1:31–2.
[28] Stejskal EO, Tanner JE. J Chem Phys 1965;42:288–92.
[29] Brereton MG. Macromolecules 1989;22:3667–74.
[30] Ries ME, Brereton MG, Klein PG, Dounis P. Polym Gels Networks 1997;5:285–305.
[31] Ries ME, Klein PG, Brereton MG, Ward IM. Macromolecules 1998;31(15):4950–6.
[32] Klein PG, Ries ME. Prog Nucl Magn Reson Spectrosc 2003;42:31–52.
[33] Alberty KA, Hogen-Esch TE, Carlotti S. Macromol Chem Phys 2005;206:1035–42.
[34] Clarson SJ, Dodgson K, Semlyen JA. Polymer 1985;26:930–4.
[35] Kirst KU, Kremer F, Pakula T, Hollingshurst J. Colloid Polym Sci 1994;272(11):1420–9.
[36] Di Marzio EA, Guttman CM. Macromolecules 1987;20(6):1403–7.
[37] Costagliola M, Greco R, Martuscelli E. Polymer 1978;19:860–2.
[38] von Meerwall E, Grigsby J, Tomich D, van Antwerp R. J Polym Sci Polym Phys Ed 1982;20(6):1037–53.
[39] Fleischer G. Colloid Polym Sci 1987;265(2):89–95.
[40] Pearson DS, Ver Strate G, von Meerwall E, Schilling FC. Macromolecules 1987;20(5):1133–41.
[41] von Meerwall E, Beckman S, Jang J, Mattice WL. J Chem Phys 1998;108:4299–304.
[42] von Meerwall E, Feick EJ, Ozisik R, Mattice WL. J Chem Phys 1999;111:750–7.
[43] Bloomfield V, Zimm BH. J Chem Phys 1966;44(1):315–23.
[44] Fleischer G, Appel M. Macromolecules 1995;28(21):7281–3.
[45] Wang S, von Meerwall ED, Wang S-Q, Halasa A, Hsu W-L, Zhou JP, et al. Macromolecules 2004;37(4):1641–51.
[46] Cheng SZD, Barley JS, von Meerwall ED. J Polym Sci Polym Phys Ed 1991;29:515–25.
[47] Macedo PB, Litovitz TA. J Chem Phys 1965;42(1):245–56.